Towards Continuous Identification of Passive Human Joint Impedance Using Physical Human-Robot Interaction System

Bilal Tout, Jason Chevrie, Antoine Dequidt, Laurent Vermeiren

Towards Continuous Identification of Passive Human Joint Impedance Using Physical Human-Robot Interaction System

Bilal Tout*, Jason Chevrie*, Antoine Dequidt*†, and Laurent Vermeiren*
*UPHF, CNRS, UMR 8201 - LAMIH, F-59313 Valenciennes, France
†INSA Hauts-de-France, F-59313 Valenciennes, France
Email: {Bilal.Tout, Jason.Chevrie, Antoine.Dequidt, Laurent.Vermeiren}@uphf.fr

***Abstract*— The identification of human joint impedance is necessary for various applications, such as improving rehabilitation efficiency or monitoring the human operator's state (fatigue, stress). To this end, in this paper we combine robot's payload identification methods with sliding window recursive least squares algorithm allowing a continuous identification of the varying human joint model without the need for external sensors. We also propose a threshold for detecting fake changes in the identified model parameters due to numerical issues. The presented approach is validated by simulations and experiments using elastic rubber bands representing a simplified passive human joint model attached to a one degree of freedom robotic system. Comparison with simple recursive least squares shows that the proposed method is promising, as it converges to the new parameter in a single window length, whereas the other method takes much longer. In addition, it distinguishes real from fake changes depending on the validity of the used model.**

I. INTRODUCTION

Human passive joint properties are commonly utilized in various fields such as rehabilitation and collaborative robotics to achieve high performance model-based control or in the clinical field to assess neuro-muscular disorders [1]. The identification of human joint impedance dynamic parameters has been widely studied in the literature. Many studies such as [2]–[6] consider an easy to identify spring-damper-mass/inertia (KBM/KBI) model to represent the human joint impedance, while others consider more complex models, such as a double exponential expression [7]–[9], which are nonlinear in the parameters and hence require more complex identification algorithms.

One method for identifying human joint impedance during physical human-robot interaction (pHRI) is to directly use human joint torques and displacements measured with external sensors such as motion capture systems and force/torque sensors as in [4]. Another method is to use only the torque estimated from the motors currents and the angles measured by the encoders at the motors shafts as in [5] and [7]. This last method requires an accurate modeling and knowledge of the robot parameters in order to obtain good identification of the human parameters. Although [5] used a second order model to represent the behavior of the robotic system, it can be better represented using the inverse dynamic model (IDM) that can be obtained using the Newton-Euler or the Lagrangian equations presented in [10]. Authors in [11] and [12] have reviewed the entire process for identifying the robot dynamic parameters as well as various identification algorithms such as ordinary least squares (OLS) and maximum likelihood estimators. Furthermore, in [13] and [14], OLS was used to identify a payload attached to an industrial robot's end-effector, using two experiments with and without the payload.

Human joint impedance depends on the state of the subject (fatigue, stress). Results in [5] and [6] showed that the ankle mechanical impedance varies during locomotion. Despite the use of time-varying identification methods in [5], the goal was to identify a system that undergoes the same time-varying behavior across each realization which is not suitable for the detection of the changes in human behavior such as fatigue. In addition, [4] and [6] identified human joint impedance in specific timing points during a task, which does not allow the detection of sudden changes in human behavior (stress, spasticity) between two timing points. Online identification methods may be a good alternative to solve this problem. Recursive least squares (RLS) algorithm [15], [16] is a commonly used one due to its simple implementation. Although the addition of a forgetting factor (or exponential window), gives RLS the ability to exponentially forget past data, the sliding window RLS (SW-RLS) algorithm performs better when processing data with sharp changes, by radically forgetting past data outside the chosen window [17]–[19].

In this paper, we propose a method combining the payload identification methods presented in [13] and the SW-RLS identification algorithm, in order to identify time-varying human joint dynamic model parameters. This method allows a continuous monitoring of the state of the human operator during pHRI using only robot joint torques and kinematic measurements without the need for external sensors. In addition, we propose a threshold-based method to allow the detection of fake changes in the identified model parameters typically arising when the trajectory does not provide sufficient excitation in the data. The proposed method is first tested in simulation to allow a comparison between estimates and ground-truth (GT) values under different noise conditions. Experimental validation is then carried out by identifying elastic rubber bands (ERBs) of known stiffness providing GT values for comparison, and simulating a simple model of a passive human operator.

This paper is organized as follows: existing and adopted human and robot models are recalled in Section II. Then identification methods are presented in Section III. Sections IV and V show simulation and experimental setups, respectively, with results and discussions for the validation of the used model and identification methods. Finally, Section VI includes the conclusion and future work.

II. SYSTEM MODELING

A. Robot Model

The inverse dynamic model (IDM) of a rigid robot with n degrees of freedom (DOF) gives the joint forces and torques $\tau_r \in \mathbb{R}^n$ as a function of joint positions, velocities and accelerations $q, \dot{q}, \ddot{q} \in \mathbb{R}^n$. It can be obtained from the Newton-Euler or the Lagrangian equations [10] as follows:

$$\tau_r = M(q) \cdot \ddot{q} + C(q, \dot{q}) \cdot \dot{q} + g(q) + f(\dot{q}), \tag{1}$$

where $M(q) \in \mathbb{R}^{n \times n}$ is the robot inertia matrix, $C(q, \dot{q}) \in \mathbb{R}^{n \times n}$ is the Coriolis and centrifugal matrix, $g(q) \in \mathbb{R}^n$ is the gravitational term, and $f \in \mathbb{R}^n$ is the friction term. Several friction models exist [20] such as the following common one:

$$f_j = F_{v_j} \cdot \dot{q}_j + F_{c_j} \cdot sign(\dot{q}_j), \tag{2}$$

with F_{v_j} and F_{c_j} the viscous and Coulomb's friction coefficients of the jth joint, respectively. The IDM in (1) can be expressed as a linear function of the standard dynamic parameters $\chi_r = \left[\chi_{r1}^T \ \chi_{r2}^T \ \cdots \ \chi_{rn}^T\right]^T \in \mathbb{R}^p$ as follows:

$$\tau_r = IDM_{\chi_r}(q, \dot{q}, \ddot{q}) \cdot \chi_r, \tag{3}$$

where $IDM_{\chi_r}\left(q, \dot{q}, \ddot{q}\right) \in \mathbb{R}^{n \times p}$ is the model regressor and χ_{rj} contains inertia parameters, first moment, mass, inertia of the actuator and friction parameters of the jth link.

The IDM (3) can be further reduced to depend only on the minimal set of base inertial parameters $\beta_r \in \mathbb{R}^{b_r}$ [21], also known as identifiable parameters [22], such that the measured torque τ_{rm} can be represented as follows:

$$\tau_{rm} = IDM_{\beta_r}(q, \dot{q}, \ddot{q}) \cdot \beta_r + e, \tag{4}$$

where $IDM_{\beta_r}(q, \dot{q}, \ddot{q}) \in \mathbb{R}^{n \times b_r}$ is the reduced model regressor and $e \in \mathbb{R}^n$ is the error due to measurement noises and modeling uncertainties present in practice.

When the robot is controlled to follow an exciting trajectory of N samples with a sampling time T_s, an over-determined linear system with $r = n \cdot N$ equations and b_r unknowns is obtained, such that

$$Y_r = W_r(q, \dot{q}, \ddot{q}) \cdot \beta_r + \epsilon, \tag{5}$$

where Y_r and $\epsilon \in \mathbb{R}^r$ are the sampled vectors of τ_{rm} and e, respectively, and $W_r(q, \dot{q}, \ddot{q}) \in \mathbb{R}^{r \times b_r}$ is the sampled matrix of $IDM_{\beta_r}(q, \dot{q}, \ddot{q})$, referred to as the observation matrix.

B. Human Model

Linear models provide a good approximation for describing joint dynamics when experimental conditions such as muscle activation level are kept relatively constant [1]. Joint dynamics have frequently been modeled using a spring-damper-inertia (KBI) model of the form

$$\tau_h = J_h \cdot \ddot{\theta}_h + B_h \cdot \dot{\theta}_h + K_h \cdot \theta_h, \tag{6}$$

where τ_h is the torque applied by the robot on the human, θ_h is the human joint angular position and $\{J_h, B_h, K_h\}$ are the human inertia, angular damping and angular stiffness parameters, respectively.

Because the human elastic equilibrium angular position θ_{h_0} is not always the constant, a better model that takes this into account can be defined as follows:

$$\tau_h = J_h \cdot \ddot{\theta}_h + B_h \cdot \dot{\theta}_h + K_h \cdot (\theta_h - \theta_{h_0}). \tag{7}$$

Both models in (6) and (7) are linear in function of human joint parameters, and can be written similarly to (5) as an over-determined linear system of N equations and b_{hi} unknowns with $i = \{1, 2\}$[1], such that

$$Y_h = W_{hi}(\theta_h, \dot{\theta}_h, \ddot{\theta}_h) \cdot \beta_{hi} + \epsilon, \tag{8}$$

where Y_h and $\epsilon \in \mathbb{R}^N$ are the sampled vectors of τ_h and e, respectively; $W_{hi}(\theta_h, \dot{\theta}_h, \ddot{\theta}_h) \in \mathbb{R}^{N \times b_{hi}}$ is the observation matrix; $\beta_{h1} = [J_h, B_h, K_h]^T \in \mathbb{R}^{b_{h1}}$ and $\beta_{h2} = [J_h, B_h, K_h, \Gamma_0]^T \in \mathbb{R}^{b_{h2}}$, with $\Gamma_0 = K_h \cdot \theta_{h0}$, are the human joint parameter vectors corresponding to models (6) and (7), respectively.

C. Human-Robot Model

In a pHRI system where the human operator is assumed to be rigidly connected to the robot's end-effector the motor torque can be expressed as follows:

$$\tau_r = M(q) \cdot \ddot{q} + C(q, \dot{q}) \cdot \dot{q} + g(q) + f(\dot{q}) + J(q)^T \cdot \tau_h, \tag{9}$$

with $J(q)$ the Jacobian of the robot such that $\dot{\theta} = J(q) \cdot \dot{q}$. Thereafter, we set $\theta = q/N_1$ as would be the case for a 1-DOF system or a n-DOF wearable robot (*i.e.* an exoskeleton) such that $J(q) = diag(1/N_j)$, with N_j being the reduction ratio of the joint j. The sampled motor torque $Y_m \in \mathbb{R}^r$ can be expressed as a function of both the robot and the human dynamics, and of only the robot joint kinematics as follows:

$$Y_m = W_r(q, \dot{q}, \ddot{q}) \cdot \beta_r + W_{hi}(q, \dot{q}, \ddot{q}) \cdot \beta_{hi} + \epsilon, \tag{10}$$

where $W_{hi}(q, \dot{q}, \ddot{q})$ is the human joint observation matrix. Furthermore, by combining human and robot dynamic parameters β_r and β_{hi} into one vector of separately identifiable parameters β_{rhi}, equation (10) can be rewritten as

$$Y_m = W_{rhi}(q, \dot{q}, \ddot{q}) \cdot \beta_{rhi} + \epsilon, \tag{11}$$

where $W_{rhi}(q, \dot{q}, \ddot{q})$ is the observation matrix of the considered human-robot interaction system.

III. PROPOSED IDENTIFICATION METHODS

We propose to combine the SW-RLS algorithm with the payload identification methods presented in [13] in order to identify the joint impedance parameters of the human user attached to the robot's end-effector.

A. Optimal Exciting Trajectory

A common way to design a persistently periodic exciting reference trajectory for the identification procedure has been proposed in [23]. It consists in optimally parameterizing a finite Fourier series function by optimizing the condition number of the corresponding observation matrix W of the model. Using the chosen Fourier series order N_{FS} and the signal time period T_p, the largest frequency f_{max} of the exciting signal can be easily calculated as $f_{max} = N_{FS}/T_p$.

[1] In the rest of the paper, index $i = \{1, 2\}$ will refer to the desired human model in equations (6) and (7) respectively.

B. SW-RLS Algorithm

In our proposed approach, the SW-RLS algorithm applies at time step $k \in [S_{win}, N]$ the OLS algorithm on filtered data in the interval $[k - S_{win} + 1, k]$, where S_{win} is the window size corresponding to a window time $T_{win} = S_{win} \times T_s$. Data filtering is done following the rules described in [24], where position data q^{win} over the window is filtered with a non-causal zero-phase low-pass Butterworth filter of cutoff frequency $f_c > 10 \times f_0$, with f_0 the natural frequency of the system. Then, the derivatives $\hat{\dot{q}}^{win}$ and $\hat{\ddot{q}}^{win}$ are calculated using a central difference algorithm of the low-pass filtered position data. In addition, a parallel decimation procedure low-pass filters in parallel the torque Y^{win} sampled over the desired window and each column of the corresponding observation matrix W^{win} using a filter of cutoff frequency $f_{c_d} > 2 \times f_0$ resulting in filtered $\hat{Y}^{win}$ and $\hat{W}^{win}$.

C. Identification Methods

In order to estimate human joint dynamic parameters, we propose to compare the integration of the SW-RLS algorithm within the four identification methods presented in [13] which were used to estimate the parameters of a payload attached to the robot's end-effector. Each of these methods requires two separate sets of experiments, one with and one without the human interacting with the robot, which will be referred to in the remainder of the paper as trajectories RH (robot-human) and R (robot alone), respectively. Correspondingly, the data obtained during each experiment is labeled RH and R, respectively. In the following a description of the modified methods is provided.

Method 1: First, estimates $\widehat{\beta}_r$ of the robot parameters β_r are obtained from data R by applying OLS algorithm to the filtered equation (5). Then, the human torque $\widetilde{Y}_h^{win}$ over a window is computed from data RH according to

$$\widetilde{Y}_h^{win} = Y_m^{win} - \widetilde{W}_r^{win}(\hat{q}^{win}, \hat{\dot{q}}^{win}, \hat{\ddot{q}}^{win}) \cdot \widehat{\beta}_r, \qquad (12)$$

where $\widetilde{W}_r^{win}(\hat{q}^{win}, \hat{\dot{q}}^{win}, \hat{\ddot{q}}^{win})$ is the robot observation matrix over a window of size S_{win} calculated from data RH. Then, estimates $\widehat{\beta}_{h_i}$ of the human parameters are obtained using the SW-RLS algorithm with the filtered human torque $\hat{\widetilde{Y}}_h^{win}$ and human observation matrix $\hat{\widetilde{W}}_{h_i}^{win}(\hat{q}^{win}, \hat{\dot{q}}^{win}, \hat{\ddot{q}}^{win})$ computed from filtered data RH. With this method, no constraints have to be imposed to the reference trajectories with and without the human.

Method 2: First, estimates $\widehat{\beta}_r$ of the robot parameters β_r are obtained in the same way as Method 1. Then, estimates $\widehat{\beta}_{rh_i}$ of the human-robot system are identified using SW-RLS algorithm with filtered data RH. Then, estimates $\widehat{\beta}_{h_i}$ of the human model are determined by subtracting the values of the corresponding robot estimates $\widehat{\beta}_r$ from those of the corresponding estimates $\widehat{\beta}_{rh_i}$ of the human-robot system. Nonetheless, attention must be paid that the full observation matrix $W_{rh_i}(q, \dot{q}, \ddot{q})$ remains well conditioned.

Method 3: It is assumed that the controller is strong enough to closely follow the reference trajectory in both R and RH trajectories. Therefore, the human torque over a window $\widetilde{Y}_h^{win}$ is computed from motor torques $Y_{m_r}^{win}$ and $Y_{m_{rh}}^{win}$ in data R and RH, respectively, according to

$$\widetilde{Y}_h^{win} = Y_{m_{rh}}^{win} - Y_{m_r}^{win}. \qquad (13)$$

Then, the human parameter estimates $\widehat{\beta}_{h_i}$ are directly identified using SW-RLS algorithm with the filtered human torque $\hat{\widetilde{Y}}_h^{win}$ and human observation matrix $\hat{\widetilde{W}}_{h_i}^{win}(\hat{q}^{win}, \hat{\dot{q}}^{win}, \hat{\ddot{q}}^{win})$ computed from filtered data RH.

Method 4: An augmented system of torque Y_{win}^{aug} and observation matrix $W_{win}^{aug}(\hat{q}^{win}, \hat{\dot{q}}^{win}, \hat{\ddot{q}}^{win})$ over a window of size S_{win} is built from the filtered motor torque measurements $\hat{Y}_{m_r}^{win}$ and $\hat{Y}_{m_{rh}}^{win}$ of data R and RH, respectively, as well as the filtered observation matrices: a) $\hat{W}_r^{win}(\hat{q}^{win}, \hat{\dot{q}}^{win}, \hat{\ddot{q}}^{win})$ of the robot computed from filtered data R, b) $\hat{\widetilde{W}}_r^{win}(\hat{q}^{win}, \hat{\dot{q}}^{win}, \hat{\ddot{q}}^{win})$ of the robot and $\hat{\widetilde{W}}_{h_i}^{win}(\hat{q}^{win}, \hat{\dot{q}}^{win}, \hat{\ddot{q}}^{win})$ of the human, both computed from filtered data RH. The augmented system is then written as

$$Y_{aug}^{win} = \begin{bmatrix} \hat{Y}_{m_r}^{win} \\ \hat{Y}_{m_{rh}}^{win} \end{bmatrix}, \qquad (14)$$

$$W_{aug}^{win} = \begin{bmatrix} \hat{W}_{r_{win}} & \mathbf{0}_{(S_{win} \times b_{h_i})} \\ \hat{\widetilde{W}}_r^{win} & \hat{\widetilde{W}}_{h_i}^{win} \end{bmatrix}. \qquad (15)$$

Then estimates $\widehat{\beta}_r$ and $\widehat{\beta}_{h_i}$ of robot and human parameters, respectively, are identified simultaneously using SW-RLS algorithm and augmented matrices Y_{aug}^{win} and W_{aug}^{win}.

D. Threshold for fake changes detection

Since the excitation trajectory is optimized taking a full period T_p into account (see Section III-A), it is not guaranteed that the trajectory remains sufficiently exciting inside the sliding windows. In order to check the validity of changes in parameters during identification with sliding windows, we define a threshold TH as follows:

$$TH = Cond(W_{ref}) \times w_{ratio}, \qquad (16)$$

where $Cond(W_{ref})$ is the condition number of the corresponding observation matrix constructed using reference trajectory signals and $w_{ratio} = N_p / S_{win}$ is the ratio between the number of data samples in one period $N_p = T_p / T_s$ and the chosen window size S_{win}. During identification using SW-RLS algorithm, results at step k are considered valid as long as the following applies:

$$Cond(W_k^{win}) < TH \qquad (17)$$

where $Cond(W_k^{win})$ is the condition number of the observation matrix constructed using data in $[k - S_{win} + 1, k]$.

IV. SIMULATION

A. System Description

The actual system depicted in Fig. 1 is a cable-driven robot joint, controlled using a PID controller implemented in a Beckhoff EL7411 driver running via TwinCAT. It is made up of a handle with a lever arm $R = 7.4\ cm$ and a mass

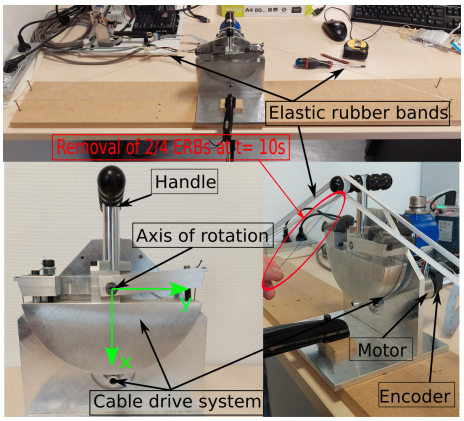

Fig. 1: System used for validation and simulation's reference.

linked by a cable (reduction ratio $N_1 = 15$) to a Maxon motor (EC-max 40mm, brushless 120W) with a HEDL 5540 encoder that measures the angular position of the motor shaft with a resolution of 500 counts per turn, corresponding to a quantization step $\delta_{quant} = 2\pi/(500 \times 4) = 0.0031416\ rad$. Measurements are acquired at a sampling period $T_s = 1\ ms$. See [25] for more details. To simulate a KBI human joint behavior, we consider ERBs interacting with the system through its handle, as illustrated in Fig. 1. In such a case, equation (1) may be expressed as follows:

$$\tau_r = J_r\ \ddot{q} + F_{v_r}\ \dot{q} + F_{c_r}\ sign(\dot{q}) + M_{x_r}\ g\ \sin\left(\frac{q}{N_1}\right) + M_{y_r}\ g\ \cos\left(\frac{q}{N_1}\right) = W_r(q, \dot{q}, \ddot{q}) \cdot \beta_r, \quad (18)$$

where $\beta_r = [M_{x_r}, M_{y_r}, F_{v_r}, F_{c_r}, J_r]^T$ with M_{x_r} and M_{y_r} the robot first moments along x and y axis, respectively, J_r the equivalent inertia of the handle and motor shaft, F_{v_r} and F_{c_r} the robot friction coefficients defined in (2) and g the gravitational acceleration. Equations (6) and (7) then become

$$\widetilde{\tau}_h = \widetilde{J}_h\ddot{q} + \widetilde{B}_h\dot{q} + \widetilde{K}_h q = W_{h_1}(q, \dot{q}, \ddot{q}) \cdot \widetilde{\beta}_{h_1}, \quad (19)$$

$$\widetilde{\tau}_h = \widetilde{J}_h\ddot{q} + \widetilde{B}_h\dot{q} + \widetilde{K}_h q - \widetilde{\Gamma}_0 = W_{h_2}(q, \dot{q}, \ddot{q}) \cdot \widetilde{\beta}_{h_2}, \quad (20)$$

where $\widetilde{\beta}_{h_1} = \left[\widetilde{J}_h, \widetilde{B}_h, \widetilde{K}_h\right]^T$ and $\widetilde{\beta}_{h_2} = \left[\widetilde{J}_h, \widetilde{B}_h, \widetilde{K}_h, \widetilde{\Gamma}_0\right]^T$ with $\widetilde{\beta}_{h_i} = \beta_{h_i}/N_1^2$. $\widetilde{\tau}_h$, $\widetilde{J}_h$, $\widetilde{B}_h$ and $\widetilde{K}_h$ denote the human torque, inertia, angular damping and angular stiffness at the motor side, respectively, and $\widetilde{\Gamma}_0 = \widetilde{K}_h \cdot N_1\theta_{h_0}$.

Initial estimates of the robot dynamic parameters, considered as ground-truth values in the simulation, were computed using parameters previously identified in [25] and the geometric characteristics of the system, leading to $\beta_{r_{GT}} = [1.518 \times 10^{-3},\ 0, 1.45 \times 10^{-4}, 2.479 \times 10^{-3}, 1.9 \times 10^{-5}]^T$. An approximation of the natural frequency $f_0 = 0.97\ Hz$ of the robotic system can be obtained from $\beta_{r_{GT}}$. Thus, cutoff frequencies $f_c = 10\ Hz > 10 \times f_0$ and $f_{c_d} = 5\ Hz > 2 \times f_0$ are chosen for the position and decimation filters.

B. Simulation Setup

To compare the proposed identification methods detailed in section III-C, the robot model (18) and human model (19) were implemented in simulation in Matlab/Simulink using the values $\beta_{r_{GT}}$ and $\widetilde{\beta}_{h_{1_{GT}}} = [0, 0, 1 \times 10^{-3}]^T$. Next, these equations were used to generate the simulation data R and RH, where $\widetilde{K}_h$ doubles its value at half the period $T_p/2$, leading to $\widetilde{\beta}^{new}_{h_{1_{GT}}} = [0, 0, 2 \times 10^{-3}]^T$. The reference trajectory was taken as a Fourier series function of order $N_{FS} = 5$ and period $T_p = 10\ s$, optimized so that the corresponding observation matrix W is well-conditioned [23]. During data generation, the position measurements were quantized using δ_{quant} of the real system, and a zero mean white Gaussian noise was added to the torque output as a measurement error. Then the simulated data R and RH were processed, using an 8^{th} order Butterworth lowpass filter of cutoff frequency $f_c = 10\ Hz$ and a 4^{th} order Butterworth decimation filter of cutoff frequency $f_{c_d} = 5\ Hz$. Finally, the processed data R and RH are used to identify robot and human model parameters with the different Methods 1-4. The data samples when velocities $|\dot{q}| < 0.1\ rad/s$ are removed form the identification procedure to avoid numerical issues due to the discontinuity in the dry friction model. Several window sizes $S_{win} = \{1000, 2000, 4000\}$ corresponding to window times $T_{win} = \{1, 2, 4\}s$ were tested to examine the effect of window size S_{win}. Results were also compared to those of RLS with different forgetting factors $\lambda = \{0.995, 0.999, 0.9995, 1\}$.

C. Simulation Results and Discussion

From Fig. 2a, showing the identification of $\widetilde{K}_h$ using model 1 and Method 1, it can be observed that after changing the value of $\widetilde{K}_h$ to $\widetilde{K}^{new}_h$ at $t = 5\ s$ the RLS estimates of $\widetilde{K}_h$ move further away from $\widetilde{K}^{new}_h$ as λ approaches 1. The delay to reach the new value also increases and the variations of

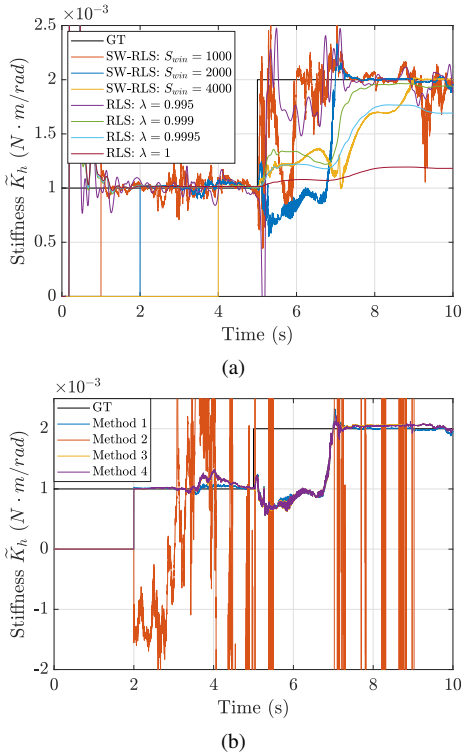

Fig. 2: Comparison of identification results of the varying stiffness $\widetilde{K}_h$ in simulation using: a) Method 1 and RLS with different values of S_{win} and λ, respectively, b) Method 1 to 4 using $S_{win} = 2000$.

the estimated parameter decreases as λ approaches 1. On the other hand, the estimates of the SW-RLS seem to converge to the value of $\widetilde{K}_h^{new}$ after T_{win} seconds, with noisy variations that increase when T_{win} decreases. It can be seen that these variations becomes significant for $T_{win} < 2\ s$, which can be explained by the fact that this value of T_{win} corresponds to the period of the largest frequency f_{max} of the excitation signal. Thus, both methods require a good choice of the values of λ or T_{win} to avoid the variations of the parameter when it is not supposed to change. However the SW-RLS method always converges to the value $\widetilde{K}_h^{new}$ within T_{win} seconds, while the RLS converge to a value quite far from $\widetilde{K}_h^{new}$ if λ is not well chosen. A trade-off choice of T_{win} is to take it larger than but close to the minimum window time $T_{win}^{min} = 1/f_{max}$. The estimates of the other parameters $\widetilde{B}_h$ and $\widetilde{I}_h$ with both methods remain around zero with noisy variations that depend on the choice of λ and S_{win} but were not illustrated for lack of space.

Results in Fig. 2b shows that Methods 1, 3 and 4 behave approximately in the same way, while Method 2 does not work at all. The poor performance of Method 2 is related to the use of a trajectory with small position amplitudes, which makes the corresponding observation matrix $W_{rh_1}(q, \dot{q}, \ddot{q})$ ill-conditioned because of the linear relationship that appears between the columns corresponding to parameters M_{x_r} and K_h. Method 3 gives good results in this case, since the R and RH trajectories are the same, and the robot follows them well. We can also notice that the different methods give parameters that are poorly estimated in some parts of the trajectory. This might be due to inaccurate modeling of the system's dynamics in these parts of the trajectory, or to the fact that the effect of some parameters on the system's dynamics vanishes in these parts due to a lack of excitation.

V. EXPERIMENTAL VALIDATION

A. Experimental Setup

To experimentally validate the proposed identification methods, ERBs were used instead of a human operator since their stiffness can be measured and used as ground-truth for validation. The linear stiffness K_L of 4 ERBs was determined experimentally by measuring with a digital dynamometer (SAUTER FC100) the forces provided by each ERB at known displacements in their linear region of operation. K_L was computed by linear fitting, yielding a mean value of $K_L = 11.61 \pm 0.69\ N/m$. The mean stiffness value is then considered the ground-truth value. Two ERBs are attached on each side of the system in order to have an elastic equilibrium angular position $\theta_{h_0} \approx 0\ rad$. K_L was then approximately converted into the equivalent angular stiffness at the motor side $\widetilde{K}_A = 4 \times K_L \times R^2/N_1^2 = 1.13 \times 10^{-3}\ N.m/rad$. However, exactly reaching $\theta_{h_0} = 0\ rad$ is not possible because of the slight asymmetry of the used ERBs. The same is likely to apply for the human since θ_{h_0} is not well defined in this case. Therefore, both human models in equations (19) and (20) were compared. Next, experimental data generation was carried out by controlling the robot to follow reference exciting trajectories, consisting of Fourier series functions of order $N_{FS} = 7$ and period $T_p = 10\ s$ leading to $T_{win}^{min} = 1.43\ s$, optimized so that the corresponding observation matrix W is well-conditioned [23]. The quantized version of the signals were included in the optimization to take into account the large quantization step of our system. In order to have a variable parameter $\widetilde{K}_h$, 2 ERBs are suddenly removed at time t while the experiment is running. Finally, the experimental R and RH data were processed, with the same filters as in Section IV-B, and used to identify the parameters of the robot and both human models using only Method 1 as it gave good results in

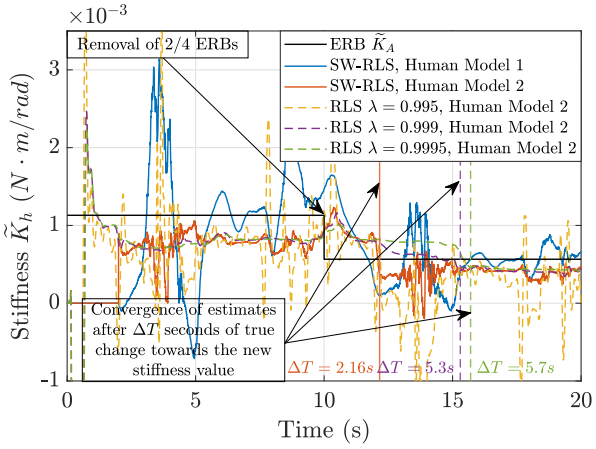

(a) Estimated stiffness $\widetilde{K}_h$ of ERBs

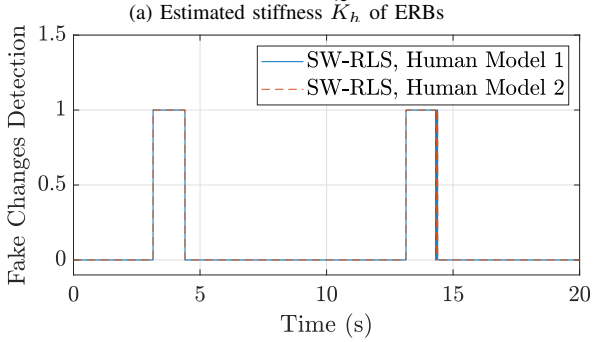

(b) Detection of fake changes using threshold TH in eq. (17)

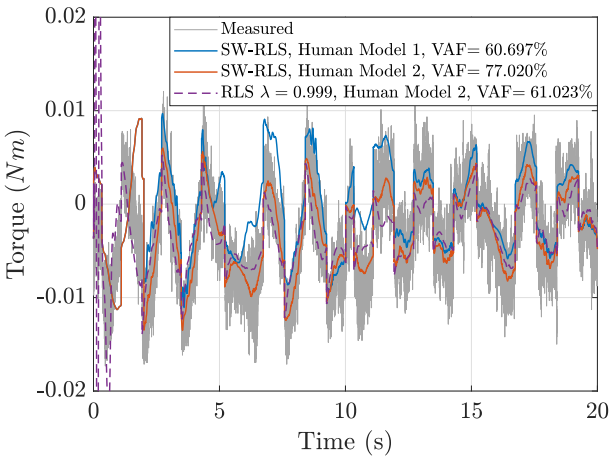

(c) Measured versus Reconstructed Torque using identified parameters.

Fig. 3: Experimental identification results of ERBs with variation of stiffness $\widetilde{K}_A$ at $t = 10\ s$ using Method 1 with $S_{win} = 2000$, and RLS with several λ comparing the human models 1 and 2 in equations (19) and (20).

simulation and a window size $S_{win} = 2000$ corresponding to $T_{win} = 2\ s > T_{win}^{min}$ in this case. Results were also compared to those of RLS with $\lambda = \{0.995, 0.999, 0.9995\}$. Variance accounted for (VAF) was used to compare the torque estimated from the identified parameters to the measured one.

B. Experimental Results and Discussion

Fig. 3a shows that $\widetilde{K}_h$ is always underestimated, mainly because the ERBs' lever arm is not kept at its maximum value, reducing the resulting torque. Hence, the efficiency of the identification algorithms will be evaluated by comparing their rate of convergence to half the average value prior to the removal of $2/4$ of the ERBs at $10\ s$. Fig. 3a shows that SW-RLS with model 2 outperforms RLS by converging in $T_{win} \approx 2\ s$ against $5.3\ s$ ($\lambda = 0.999$) and $5.7\ s$ ($\lambda = 0.9995$). In contrast, both SW-RLS with model 1 and RLS with $\lambda = 0.995$ converge after $2\ s$, but with significant noisy variations. Fig. 3b shows the detection of ill-conditioning of the observation matrix according to the threshold TH defined in (16). It can be seen that when using model 2 this threshold allows the detection of fake changes in the estimates in intervals $t = \{3, 4.5\}\ s$ and $t = \{13, 14.5\}\ s$. On the other hand, the parameters estimated with model 1 present large variations that are not detected as fake changes using TH. This is certainly due to the fact that model 2 gives a better representation of the system. So the proposed threshold TH allows a detection of fake changes of the estimated parameters as long as modeling errors are small enough. Finally, we can observe in Fig. 3c that the measured torque is better reconstructed using SW-RLS estimates with model 2 (VAF= 77.02%) than with model 1 (VAF= 60.697%) or using RLS with $\lambda = 0.999$ (VAF= 61.023%).

VI. CONCLUSION AND FUTURE WORKS

This paper combines robot's payload identification methods with sliding window recursive least squares algorithm to continuously identify the dynamic parameters of a human-robot interaction system. A threshold for detecting fake changes in the identified parameters in case of insufficient excitation is also proposed. The proposed approach is compared with recursive least squares algorithm, both in simulation and on a one degree of freedom robotic system using elastic rubber bands to imitate the human part. Results show that the proposed approach can overcome recursive least squares in terms of convergence rate and precision and can enable distinguishing real from fake changes in the parameters, with varying performance depending on the accuracy of the used model. Future works include: 1) the improvement of the optimal exciting trajectory allowing the use of smaller window sizes to achieve faster convergence, 2) the use of adaptive window sizes to ensure good conditioning, 3) the test of the proposed methods with a real human interacting with the robotic system to study the inter/intra-subject variation of human parameters.

REFERENCES

[1] R. E. Kearney and I. W. Hunter, "System identification of human joint dynamics," *Crit. Rev. in Biomed. Eng.*, vol. 18, no. 1, Feb 1990.

[2] I. Nazon, Yves F., R. M. Doshi, and E. J. Rouse, "Validation of methods for estimation of knee joint mechanical impedance during locomotion using a torque-controllable knee exoskeleton," *J. Biomechanical Eng.*, vol. 144, no. 4, 12 2021.

[3] D. Chang, J. Hunt, J. Atkins, and H. Lee, "Validation of a novel parallel-actuated shoulder exoskeleton robot for the characterization of human shoulder impedance," in *Proceedings 2021 ICRA. IEEE International Conference on Robotics and Automation*, 2021, pp. 10 580–10 586.

[4] V. Fortineau, M. Makarov, P. Rodriguez-Ayerbe, and I. A. Siegler, "Towards a seamless experimental protocol for human arm impedance estimation in an interactive dynamic task," in *2021 30th IEEE International Conference on Robot & Human Interactive Communication (RO-MAN)*, 2021, pp. 31–36.

[5] H. Lee and N. Hogan, "Time-varying ankle mechanical impedance during human locomotion," *IEEE Trans. Neural Syst. Rehab. Eng.*, vol. 23, no. 5, pp. 755–764, 2015.

[6] E. J. Rouse, L. J. Hargrove, E. J. Perreault, and T. A. Kuiken, "Estimation of human ankle impedance during the stance phase of walking," *IEEE Trans. Neural Syst. Rehab. Eng.*, vol. 22, no. 4, pp. 870–878, 2014.

[7] Y. Li, X. Guan, W. Li, B. Penzlin, K. Liu, Z. Yang, B. Liu, S. Leonhardt, and L. Ji, "Dynamic parameter identification of a human-exoskeleton system with the motor torque data," *IEEE Trans. Medical Robot. Bionics*, vol. 4, no. 1, pp. 206–218, 2022.

[8] T. Edrich, R. Riener, and J. Quintern, "Analysis of passive elastic joint moment in paraplegics," *IEEE Trans. Biomed. Eng.*, vol. 47, no. 8, pp. 1058–1065, 2000.

[9] B. Hwang and D. Jeon, "A method to accurately estimate the muscular torques of human wearing exoskeletons by torque sensors," *Sensors*, vol. 15, no. 4, pp. 8337–8357, 2015.

[10] W. Khalil and E. Dombre, "Dynamic modeling of serial robots," in *Modeling, Identification and Control of Robots*, W. Khalil and E. Dombre, Eds. Oxford: Butterworth-Heinemann, 2002, ch. 9, pp. 191–233.

[11] Q. Leboutet, J. Roux, A. Janot, J. R. Guadarrama-Olvera, and G. Cheng, "Inertial parameter identification in robotics: A survey," *Appl. Sci.*, vol. 11, 2021.

[12] J. Wu, J. Wang, and Z. You, "An overview of dynamic parameter identification of robots," *Robot. and Computer-Integrated Manufact.*, vol. 26, no. 5, pp. 414–419, 2010.

[13] W. Khalil, M. Gautier, and P. Lemoine, "Identification of the payload inertial parameters of industrial manipulators," in *Proceedings 2007 ICRA. IEEE International Conference on Robotics and Automation*, 2007, pp. 4943–4948.

[14] C. Gaz and A. De Luca, "Payload estimation based on identified coefficients of robot dynamics — with an application to collision detection," in *2017 IEEE/RSJ International Conference on Intelligent Robots and Systems (IROS)*, 2017, pp. 3033–3040.

[15] M. Ferro, C. Gaz, M. Anzidei, and M. Venditteli, "Online needle-tissue interaction model identification for force feedback enhancement in robot-assisted interventional procedures," *IEEE Trans. Medical Robot. Bionics*, vol. 3, no. 4, pp. 936–947, 2021.

[16] A. Kurdas, M. Hamad, J. Vorndamme, N. Mansfeld, S. Abdolshah, and S. Haddadin, "Online payload identification for tactile robots using the momentum observer," in *Proceedings 2022 ICRA. IEEE International Conference on Robotics and Automation*, 2022, pp. 5953–5959.

[17] M. G. Bellanger, "The family of fast least squares algorithms for adaptive filtering," in *Numerical Linear Algebra, Digital Signal Processing and Parallel Algorithms*, G. H. Golub and P. Van Dooren, Eds. Berlin, Heidelberg: Springer Berlin Heidelberg, 1991, pp. 1–18.

[18] K. Yoo and H. Park, "Fast residual computation for sliding window recursive least squares methods," *Sig. Process.*, vol. 45, no. 1, pp. 85–95, 1995.

[19] Q. Zhang, "Some implementation aspects of sliding window least squares algorithms," *IFAC Proceed. Vol.*, vol. 33, no. 15, pp. 763–768, 2000.

[20] E. Madsen, O. S. Rosenlund, D. Brandt, and X. Zhang, "Comprehensive modeling and identification of nonlinear joint dynamics for collaborative industrial robot manipulators," *Control Eng. Pract.*, vol. 101, p. 104462, 2020.

[21] H. Mayeda, K. Yoshida, and K. Osuka, "Base parameters of manipulator dynamic models," *IEEE Trans. Robot. Automat.*, vol. 6, pp. 312–321, June 1990.

[22] C. G. Atkeson, C. H. An, and J. M. Hollerbach, "Estimation of inertial parameters of manipulator loads and links," *Int. J. Robot. Res.*, vol. 5, pp. 101–119, 1986.

[23] J. Swevers, C. Ganseman, D. Tukel, J. de Schutter, and H. Van Brussel, "Optimal robot excitation and identification," *IEEE Trans. Robot. Automat.*, vol. 13, pp. 730–740, Oct. 1997.

[24] M. Gautier, "Dynamic identification of robots with power model," in *Proceedings 1997 ICRA. IEEE International Conference on Robotics and Automation*, vol. 3, 1997, pp. 1922–1927.

[25] Q.-V. Dang, "Conception et commande d'une interface haptique à retour d'effort pour la cao," Ph.D. dissertation, Univ. de Valenciennes et du Hainaut-Cambresis, Valenciennes, Dec. 2013. [Online]. Available: https://tel.archives-ouvertes.fr/tel-00985356